Prioritize biologically relevant ions for data-independent acquisition (BRI- DIA) in LC-MS/MS-based lipidomics analysis

Likun Duan
North Carolina State University
Grace Scheidemantle
North Carolina State University
Mareca Lodge
North Carolina State University
Magdalina J Cummings
North Carolina State University
Eva Pham
North Carolina State University
Xiaoqiu Wang
North Carolina State University
Arion Kennedy
North Carolina State University
Xiaojing Liu (xliu68@ncsu.edu)
North Carolina State University

Research Article

Keywords:

Posted Date: April 25th, 2022

DOI: https://doi.org/10.21203/rs.3.rs-1585328/v1

Prioritize biologically relevant ions for data-independent acquisition (BRI-DIA) in LC-MS/MS-based lipidomics analysis

Likun Duan[1,#], Grace Scheidemantle[1,#], Mareca Lodge[1], Magdalina J Cummings[2,3], Eva Pham[1], Xiaoqiu Wang[2,3], Arion Kennedy[1], and Xiaojing Liu[1,*]

[1] Department of Molecular and Structural Biochemistry, North Carolina State University, Raleigh, NC 27695 USA

[2] Department of Animal Science, North Carolina State University, Raleigh, NC 27695 USA

[3] The Comparative Medicine Institute, North Carolina State University, Raleigh NC 27695, USA

[#] Equal contributions

[*] Corresponding author: Xiaojing Liu, xliu68@ncsu.edu

Abstract

Introduction Data-dependent acquisition (DDA) is the most commonly used MS/MS scan method for lipidomics analysis on orbitrap-based instrument. However, MS instrument associated software decide the top N precursors for fragmentation, resulting in stochasticity of precursor selection and compromised consistency and reproducibility. We introduce a novel workflow using biologically relevant lipids to construct inclusion list for data-independent acquisition (DIA), named as BRI-DIA workflow.

Objectives To ensure consistent coverage of biologically relevant lipids in LC-MS/MS-based lipidomics analysis.

Methods Biologically relevant ion list was constructed based on LIPID MAPS and lipidome atlas in MS-DIAL 4. Lipids were extracted from mouse tissues and used to assess different MS/MS scan workflow (DDA, BRI-DIA, and hybrid mode) on LC-Orbitrap Exploris 480 mass spectrometer.

Results DDA resulted in more MS/MS events, but the total number of unique lipids identified by three methods (DDA, BRI-DIA, and hybrid MS/MS scan mode) is comparable (580 unique lipids across 44 lipid subclasses in mouse liver). Major cardiolipin molecular species were identified by data generated using BRI-DIA and hybrid methods and allowed calculation of cardiolipin compositions, while identification of the most abundant cardiolipin CL72:8 was missing in data generated using DDA method, leading to wrong calculation of cardiolipin composition.

Conclusion The method of using inclusion list comprised of biologically relevant lipids in DIA MS/MS scan is as efficient as traditional DDA method in profiling lipids, but offers

better consistency of lipid identification, compared to DDA method. This study was performed using Orbitrap Exploris 480, and we will further evaluate this workflow on other platforms, and if verified by future work, this biologically relevant ion fragmentation workflow could be routinely used in many studies to improve MS/MS identification capacities.

Introduction

Due to the advances of mass spectrometers, lipidomic-focused database and software, and increasing knowledge of lipidomic pathways, lipidomics has become an emerging tool for lipidomic profiling on a large scale under physiological and pathological conditions[1-8]. The outcome of lipidomics analysis helps to understand the role of lipidomic rewiring under different conditions, generate new hypotheses, identify potential disease biomarkers, and elucidate drug mechanisms[9-13]. There is also increasing interest in advancing clinical lipidomics[6, 14-16], which aims to establish the connection of patient lipid profiles and clinical phenotypes using research-based lipidomics analysis workflow. To achieve this goal, it is important to perform lipidomics analysis with consistent lipid identification and measurement.

MS/MS scan is important in lipid identification, since MS/MS spectra not only help to identify lipid classes but also side acyl chain compositions. Data-dependent acquisition (DDA) is used frequently for lipidomics analysis on an orbitrap-based instrument[17]. However, since the precursor ion selection is influenced by sample and instrumentation condition, situations exist when lipids are detected in full scan mode with decent signals, but no MS/MS information is available for identification[8, 18]. Hence, the reproducibility of DDA method is not always satisfactory. To tackle this issue, data-independent acquisition (DIA) methods have been developed to fragment all ions within a large mass range[3, 7, 19-21]. The implementation of DIA methods has been demonstrated in various LC-MS platforms. For example, sequential window acquisition of all theoretical mass spectra (SWATH-MS) on Q-TOF mass spectrometer was described for proteomics

analysis[20] and is also being widely used for lipidomics analysis[19]. All-ion fragmentation (AIF) acquisition on Orbitrap mass spectrometer, which applies a Higher-energy Collisional Dissociation (HCD) fragmentation to all ionized molecules, is also being used[22]. These DIA methods are demonstrated to improve the consistency of identification and coverage capabilities. However, SWATH and AIF methods also have disadvantages. The broad range of precursors in these methods determines the multiplexed nature of MS/MS spectra, making it difficult to trace fragmentation ions back to their precursors as they may result from multiple precursor ions, and increasing the complexity of data analysis[3]. Further improvements in algorithms and software will be needed for deconvoluting the complexity of SWATH and AIF data[19]. DIA triggered by an inclusion list containing all the masses of a broad range with 1 Da intervals was employed in a shotgun lipidomics platform for high throughput analysis of plasma lipids[23]. Hybridizing DDA and DIA modes is trending in proteomics and metabolomics study[24-27], but has not been well adapted in lipidomics study[25].

LC-MS/MS-based lipid identification is often achieved by searching against lipid libraries or reference databases (e.g., LipidBank, LIPID MAPS, LipidBlast library, etc)[28-30]. LIPID MAPS is an experimentally and computationally-generated database, containing biologically relevant lipid species, and plays an essential role in the lipidomics field. LipidBlast is in silico MS/MS library and frequently used by lipidomics analysis software tools such as MS-DIAL. However, ions not included in the database will be unidentified, even if the MS/MS spectra are available. Therefore, in this study, we chose to prioritize the precursor ions for MS/MS scan to ensure that ions in lipid databases are fragmented when present in samples. A previous study using MS-DIAL 4 reported a comprehensive

lipidome atlas of lipids detected in different types of tissues[2]. We took advantage of such information and described a novel workflow to perform DIA MS/MS scan on Orbitrap mass spectrometer using biologically relevant lipid inclusion list (BRI-DIA). This list was built to include major lipids present in the prominent database (e.g., LIPID MAPS and or LipidBlast library)[2, 28, 29]. Based on the lipidome atlas in MS-DIAL 4, this list was further narrowed down to include lipids expected to be present in a particular sample type (e.g., mammalian tissue), depending on the focus of studies. Retention time window for each lipid subclass was determined based on standard compounds and lipids tentatively identified in full scan spectra. BRI-DIA method allowed selection of precursor ions within a narrow *m/z* range and the given time window, and hence, the resulting MS/MS spectra were less multiplexed compared to SWATH or AIF methods. We then compared the performance characteristics of DDA and BRI-DIA in lipidomics analysis of mouse tissues. These efforts are expected to decrease the stochasticity of precursor selection in MS/MS scan and ensure consistent lipid coverage, which we believe is important for many studies, especially long-term cohort study and clinical applications where samples will be analyzed in different batches over a long period of time.

Materials and methods

Reagents

Optima LC-MS grade of ammonium formate, formic acid, water, acetonitrile, isopropanol, and methanol were purchased from Fisher Scientific. HPLC grade ethyl acetate was purchased from Millipore Sigma. Methyl tert-butyl ether (MTBE) was

purchased from Acros Organics. The following lipid standards were obtained from Avanti Polar Lipids: 15:0-18:1(d7) PC, 15:0-18:1(d7) PE, 15:0-18:1(d7) PS, 15:0-18:1(d7) PG, 15:0-18:1(d7) PI, 15:0-18:1-d7-PA, 18:1(d7) LPC, 18:1(d7) LPE, 18:1(d7) Chol Ester, 18:1(d7) MG, 15:0-18:1(d7) DG, 15:0-18:1(d7)-15:0 TG, 18:1(d9) SM, and Cholesterol (d7).

Animal Models

C57BL/6 mice were housed North Carolina State University Biological Resources Facility with ad libitum access to food (Laboratory Rodent Diet 5001) and water on a 12-hour light/dark cycle. Mice were sacrificed at the age of 8-16 weeks. Tissues were immediately snap-frozen in liquid nitrogen, except that intestines were rinsed in and stored in -80 °C freezer until further analysis. All animal procedures were approved by the Institutional Animal Care and Use Committee (IACUC) at North Carolina State University.

Construction of biologically relevant inclusion list

Using LIPID MAPS and MS-DIAL 4 as the primary sources[2, 29], we built an inclusion list for MS/MS scan through few steps (Fig. 1): 1) download files of each lipid subclass from LIPID MAPS and further organize by merging structural isomers into one entity and removing lipids with molecular weight lower than 200 or higher than 1600 (*m/z*, due to scan range setup); 2) for lipid classes containing much more lipids in MS-DIAL 4[2] than LIPID MAPS, MS-DIAL results were included to increase the coverage; 3) use data generated by LC-MS methods described in the method section to determine the preferred ion type (dominant adduct ions) and retention time window of each lipid subclass (based on MS1 feature); 4) find the optimal collision energy by varying

collision energy from 10 to 35. Through these efforts, we constructed an inclusion list (Supplementary table 1) for MS/MS scan, and this list includes 1) chemical formula, 2) preferred adduct ions, 3) scheduled retention time window for MS/MS scan, and 4) preferred collision energy. Mass list used in this study is described in Supplementary table 1.

HPLC method

Lipid analysis was performed using Vanquish UHPLC (Thermo Fisher Scientific). A reversed phase chromatography method with Xbridge BEH C18 column (2.1× 100 mm, Column XP; Waters) was used for compound separation at 40 °C. Mobile phase A: water:acetonitrile (8:2, v/v) with 0.1% formic acid and 10 mM ammonium formate, and mobile phase B: isopropanol:acetonitrile (9:1, v/v) with 0.1% formic acid and 10 mM ammonium formate. Linear gradient was: 0 min, 40% B; 1.5 min, 40% B; 5.0 min, 85% B; 12.0 min, 97% B; 16.0 min, 97% B; 16.5 min, 40% B; 21.0 min, 40% B. The flow rate was: 0.15 ml/min.

Mass Spectrometry

Lipid analysis was performed on Orbitrap Exploris 480 mass spectrometer (Thermo Fisher Scientific), which was equipped with a HESI probe and operated in the positive/negative switching mode. The relevant parameters were as listed: vaporizer temperature, 350 °C; ion transfer tube temperature, 300 °C; sheath gas, 35; auxiliary gas, 7; sweep gas, 1; spray voltage, 3.5 kV for positive mode and 2.5 kV for negative mode; RF-lens (%), 45. The resolution was set at 120,000 (at m/z 200). The scan range was 200 to 1600 (*m/z*). Automatic maximum injection time (max IT) and automatic gain control (AGC) were used. MS/MS scan was acquired using three workflow (Fig. 2): 1)

DDA, 2) BRI-DIA, and 3) Hybrid mode (BRI-DIA followed by DDA). When DDA was performed, the MS instrument automatically determines the top N precursors for fragmentation one after the other. When BRI-DIA was operated, the inclusion list containing precursor ions in positive and negative ion mode was described in the Supplementary table 1. The MS/MS (for all three methods) condition for positive or negative ion mode was set as follows: precursor isolation window was set at 1 (*m/z*), HCD collision energy was set at 25%, orbitrap resolution of full scan and MS/MS scan was set at 60,000 and 15,000, respectively. Intensity threshold for DDA and DIA MS/MS scan was set at 10,000. Dynamic exclusion in DDA method was set to use automatically determined parameters.

Lipid extraction from mouse tissues and sample preparation for LC-MS analysis

All tissue sample was first homogenized in liquid nitrogen and then 10-20 mg tissues were weighed into a new 1.7 ml Eppendorf tube. Ice cold extraction solvent (400 μl 80% methanol/water) was added to each sample, and Geno/Grinder homogenizer was used (1500 rpm, 1 to 2 min) to further break down the tissue chunk and form an even suspension. 200 ul supernatant containing polar metabolites was removed after centrifugation at 20,000 g at 4 °C for 10 min. 480 μl MTBE and 10 μl internal standard solution were added to the rest samples (200 μl solvent and insoluble pellet). Water bath sonicator and vortex mixer were used to better mix the bottom pellet with extraction solvent. Finally, 120 μl water was added to initiate phase separation. All samples were centrifuged at 20,000 g at 4 °C for 10 min. The supernatant containing lipids was transferred to a new Eppendorf tube and dried using speed vacuum. The dry pellets

were reconstituted into 300 μl sample solvent (isopropanol: ethyl acetate, 1:1, v/v), and 3 μl was injected to LC-HRMS.

Data analysis

LC-MS peak extraction and integration were performed using MS-DIAL with default settings. Integrated peak area of lipids was used to calculate lipid subclass (e.g., cardiolipins) composition. Graphs were generated using GraphPad Prism 8 unless otherwise noted.

Merging or removal of lipid identities

Lipids identified by MS-DIAL were exported and subjected to further processing: 1) Mass error was calculated in an excel sheet and ions with mass error larger than 4 ppm were excluded from further analysis; 2) In addition, there were redundant lipid identifications in the result of MS-DIAL analysis. For example, there were two features with exactly the same name, similar MS/MS, and their retention time difference was less than 0.1 min. There were few potential reasons why they were listed as two lipids identified by MS-DIAL. MS/MS of the same lipid ions may be collected multiple times at slightly different time. Furthermore, the current LC-MS/MS workflow doesn't determine acyl chain positions or the location of double bonds, so these could be unresolved lipid isomers. In this study, these redundant species are merged into one identity; 3) Certain classes of lipids were detected in different ion adduct forms (e.g., $[M+H]^+$, $[M+Na]^+$, $[M-H]^-$, $[M-2H]^{2-}$, etc), and the ion form with higher signal was kept and the other ion forms were removed; 4) Under our experimental conditions, certain classes of lipids do not fragment well, such as free fatty acids (FA), N-acylethanolamine (NAE). Since the major focus of this study is to compare the performance characteristics of different MS/MS

scan method, FA and NAE lipids were removed from the final list; 5) RIKEN lipid species were also removed because there is limited knowledge available regarding their biological functions.

Results

Construction of biologically relevant lipid ion list for DIA MS/MS scan

To build a list of biologically relevant ions for DIA method, we relied on two sources: LIPID MAPS and lipidome atlas in MS-DIAL 4[2, 29]. MS-DIAL contains MS/MS spectral libraries of lipids common in mammals and others, and the classifications of these lipids followed the LIPID MAPS definition, making it easy to combine lipids from both sources. Using LIPID MAPS and MS-DIAL 4 as the primary sources, we built an inclusion list for MS/MS scan (Fig. 1). The details were described in the method section. The inclusion list (Supplementary table 1) for MS/MS scan includes 1) chemical formula, 2) preferred adduct ions, 3) scheduled retention time window for MS/MS scan, and 4) preferred collision energy.

Performance evaluation of DDA, BRI-DIA and hybrid methods in lipid identification

To compare the performance of DDA, BRI-DIA, and hybrid MS/MS methods (BRI-DIA followed by DDA), we ran the same liver extract sample three times using three methods. The parameters of each method are described in the method section. All data were processed by MS-DIAL using the software default parameter settings. Collision energy has a big impact on lipid fragmentation patterns and hence, affects lipid

identifications (data not shown). Under our experimental condition, HCD collision energy of 25% generates fragment ions which matches well with in silica MS/MS spectra in MS-DIAL. Hence, we chose this collision energy in all three methods.

Since mass error of internal standards across the entire LC-MS experiment is less than 4 ppm (Supplementary figure 1), we removed lipids identified by MS-DIAL but with mass error bigger than 4ppm. In addition, lipids identified with MS-DIAL were further reviewed to merge redundant lipid identities and remove lipid classes with poor fragmentations (e.g., free fatty acids and N-acylethanolamine). As expected, the total number of precursor ions with MS/MS spectra in data generated using DDA method is higher than DIA methods (Table 1). However, these identified lipids need further review for few reasons: 1) Some lipids were identified by MS-DIAL, but mass error (the difference between the measured and the theoretical *m/z* of that ion) is greater than 4 ppm; 2) There are redundant lipid identifications in data generated by three methods. Some precursor ions are the same lipids of different adduct ion forms; 3) Even though identified by MS-DIAL, certain classes of lipids do not fragment well, such as free fatty acids (FA), N-acylethanolamine (NAE), because the identification is entirely based on full scan MS, instead of MS/MS. The percentage of MS-DIAL identified lipids with big mass error, redundant identification, wrong retention time, and poor fragmentation information is higher in DDA data than data generated using BRI-DIA or hybrid method (Table 1). After the removal of wrong and redundant lipid identifications, the three methods detected similar numbers of lipids: 576 to 584 unique lipids across more than 21 lipid classes in mouse liver (Tables 1-3). Lipidomics results directly exported from MS-DIAL were included in Supplementary table 2.

Evaluation of lipid identification consistency in different biological samples

To evaluate the lipid identification consistency, we used cardiolipins as an example. Cardiolipins (CLs) are important lipids located on mitochondrial inner membranes. Abnormalities in CL acyl chain composition have been associated with various diseases[31]. In addition, CL composition is also tissue-specific[31]. Among all CL species, CL $(18:2)_4$ (or CL 72:8) is shown to be the dominant one. Consistent with that, CL 72:8 $[M-H]^-$ was found in full-scan mass spectra in negative ion mode. Surprisingly, MS/MS spectra of CL72:8 $[M-H]^-$ was missing in DDA data, and hence, no identification information was available for MS-DIAL to identify CL 72:8 (Fig. 3). CL 72:6 $[M-H]^-$ was selected for MS/MS scan, even though the precursor ion intensity of CL 72:6 $[M-H]^-$ is three times lower than CL 72:8 $[M-H]^-$. On the contrary, BRI-DIA using inclusion list selected and fragmented CL 72:8 $[M-H]^-$, resulting in the successful annotation of CL 72:8 by MS-DIAL. Five CL species were identified with DDA, but not BRI-DIA or hybrid method (Fig. 3). However, all five CLs were low in abundance and less than 1% of total CL species. To further evaluate the reproducibility of BRI-DIA method, we tested lipid extract from different tissue types and then plotted CL species identified in these data. As shown in Fig. 4, 55 CL molecular species were identified in liver, heart, intestine (jejunum), muscle and uterus, with a variable CL composition. CL 72:8 and CL 72:7 were dominant in mouse liver, CL 72:8, 72:7, 76:11 and 76:12 were the major species in mouse heart, and CL 72:6, 72:7, 72:8, 76:11 and 76:12 were dominant in skeletal muscle. These results (Fig. 4) were comparable to the results published elsewhere[32-34], except that the CL composition in mouse uterus was not reported yet.

Evaluation of lipid isomer identification capacities for ions with poor signals or poor chromatography

In BRI-DIA mode, MS/MS spectra were collected continuously and hence, multiple scans across a peak were obtained even for ions with poor signals. Here, we evaluated whether MS/MS spectra offered advantages in identifying isomers which shared the same *m/z* and were not well chromatographically separated. As shown in Fig. 5, we used phosphatidylinositol (PI) 37:5 as an example. 241.0119 is the theoretical m/z of the polar head group [phosphoinositol – H_2O – H]$^-$. 303.2330 or 301.2173 is the theoretical m/z of C20:4 or C20:5 negative ion. MS/MS spectra collected using BRI-DIA method suggested a mixture of PI 17:1/20:4 and PI 17:0/20:5, while there was only one MS/MS scan in DDA data corresponding to PI 17:1/20:4. We demonstrated that two LC-MS-unresolved isomers were identified based on DIA data, while in DDA data, only one MS/MS scan was collected for these isomers and hence, only one isomer was identified.

Discussion

DDA method is widely used for lipidomics analysis on orbitrap-based mass spectrometer, since it is convenient to set up and doesn't require prior knowledge of precursor ions present in samples. However, the precursor ion selection is influenced by samples and instrumentation condition, resulting in inconsistent lipid coverage[3]. DDA data also tend to comprise lipids of different adduct ions, or charge states, leading to redundant identifications when these adduct patterns are not used for complementary identification. In this study, we demonstrated a workflow to construct a biologically

relevant inclusion list and use this list for DIA MS/MS scan on an orbitrap-based mass spectrometer, Orbitrap Exploris 480. We then compared the performance of traditional DDA, DIA using inclusion list and hybrid mode. DDA resulted in the highest number of MS/MS events, but the identified lipid number is comparable to DIA and hybrid mode. Furthermore, compared to other DIA methods (e.g., SWATH, AIF, etc), this BRI-DIA method avoids multiplexed MS/MS spectra by choosing precursor ions within a narrow m/z of 1 at a given time window. BRI-DIA method offers additional advantages:

1) For the same lipid subclass, DDA tends to result in lipids of multiple ion forms. For example, many DGs were identified by MS-DIAL as their sodium (Na^+) adduct, but when we take a closer look at the MS/MS spectrum, MS-DIAL-based MS/MS spectrum for $[DG+Na]^+$ adduct provided little fragment information, and hence, compromised the accuracy of DG identification. Our inclusion list included $[DG+NH_4]^+$ but not Na adduct, and hence, the BRI-DIA data mainly contained $[DG+NH_4]^+$. For DGs, NH_4^+ adduct was more abundant than $[DG+Na]^+$ and also had more detailed fragment information in MS-DIAL MS/MS spectrum library.

2) We then further evaluated the reproducibility of three methods by performing lipidomics analysis of different tissue types and the results suggest that the use of inclusion list identified major cardiolipin species, while DDA missed few abundant cardiolipin species. The overall cardiolipin identified using BRI-DIA or hybrid mode is comparable to previous publications.

3) MS/MS spectra of the same precursor ions are collected multiple times across a peak in DIA mode, while DDA scan doesn't collect MS/MS spectra of the same precursor ions continuously and can miss isomers (Fig. 5). This is especially important for lipids with

weak signals or poorly separated chromatographically. Under such situation, DIA method can have advantage over DDA in identifying unresolved isomers.

Despite the advantage of DIA using biological relevant inclusion list, limitations exist. The current LC-MS/MS workflow doesn't determine acyl chain positions or the location of double bonds and hence isomers which differ by locations of acyl chain or double bonds are unresolved. Other separation approaches such as ion mobility or chiral chromatography have been demonstrated elsewhere for separation of these isomeric lipids[35-38]. In this study, a generic inclusion list was constructed and applied to samples from different tissues. However, some lipids may be only detected in certain tissues, but not others. Hence, if needed, a more tailored inclusion list may be developed for a particular sample type, which will make the inclusion list more targeted and focused on lipids relevant to a particular sample of interest. Furthermore, in this study we only tested this workflow on Orbitrap Exploris 480, and in future we will test this DIA workflow on other orbitrap-based mass spectrometers, such as Q Exactive Plus to see whether it is applicable or not.

Conclusion

BRI-DIA method using inclusion list comprised of biologically relevant lipids of their optimized ion forms on Orbitrap mass spectrometer, Orbitrap Exploris 480, reduced the redundancy and improved the consistency of lipid identification, compared to DDA MS/MS scan methods. We will further evaluate this workflow on other platforms, and if

verified by future work, this BRI-DIA workflow could be routinely used in many studies to improve LC-MS/MS-based lipid identification capacities.

Declarations

Ethics approval and consent to participate

All animal procedures were approved by the Institutional Animal Care and Use Committee (IACUC) at North Carolina State University.

Consent for publication

All authors have read and approved the manuscript.

Availability of data and materials

The data is available upon request from the corresponding author.

Competing interest

Authors declare that they have no conflicts of interest with the contents of this article.

Funding

This work was supported by Chemistry of Life pilot funds and startup funds (L.D., G.S., M.L., X.L., A.K.) at North Carolina State University (NCSU), National Institutes of Health 1R21DK128678-01A1 (A.K.), Center for Human Health and the Environment Pilot Project Program Award (ES025128 to X.W.) at NCSU and Animal Reproduction Program (no. 2022-67015-36491 to X.W.) from the USDA National Institute of Food and Agriculture.

Author contributions

A.K., X.W., M.L, and M.C. performed all animal experiments. G.S., L.D., and X.L. prepared samples and performed LC-MS analysis. X.L., L.D., G.S., A.K., and X.W. participated in experimental design. X.L, L.D., and G.S. interpreted results and wrote the manuscript. E.P. helped with text editing. All authors provided input on the manuscript.

Acknowledgments

We thank support from Molecular Education, Technology and Research Innovation Center (METRIC) at North Carolina State University.

Abbreviations

LC: Liquid chromatography

HRMS: High-resolution mass spectrometer

SWATH: Sequential window acquisition of all theoretical fragment ion spectra

AIF: All-ion fragmentation

DDA: Data-dependent acquisition

DIA: Data-independent acquisition

BRI: Biologically relevant ions

CL: Cardiolipin

Figure and figure legend

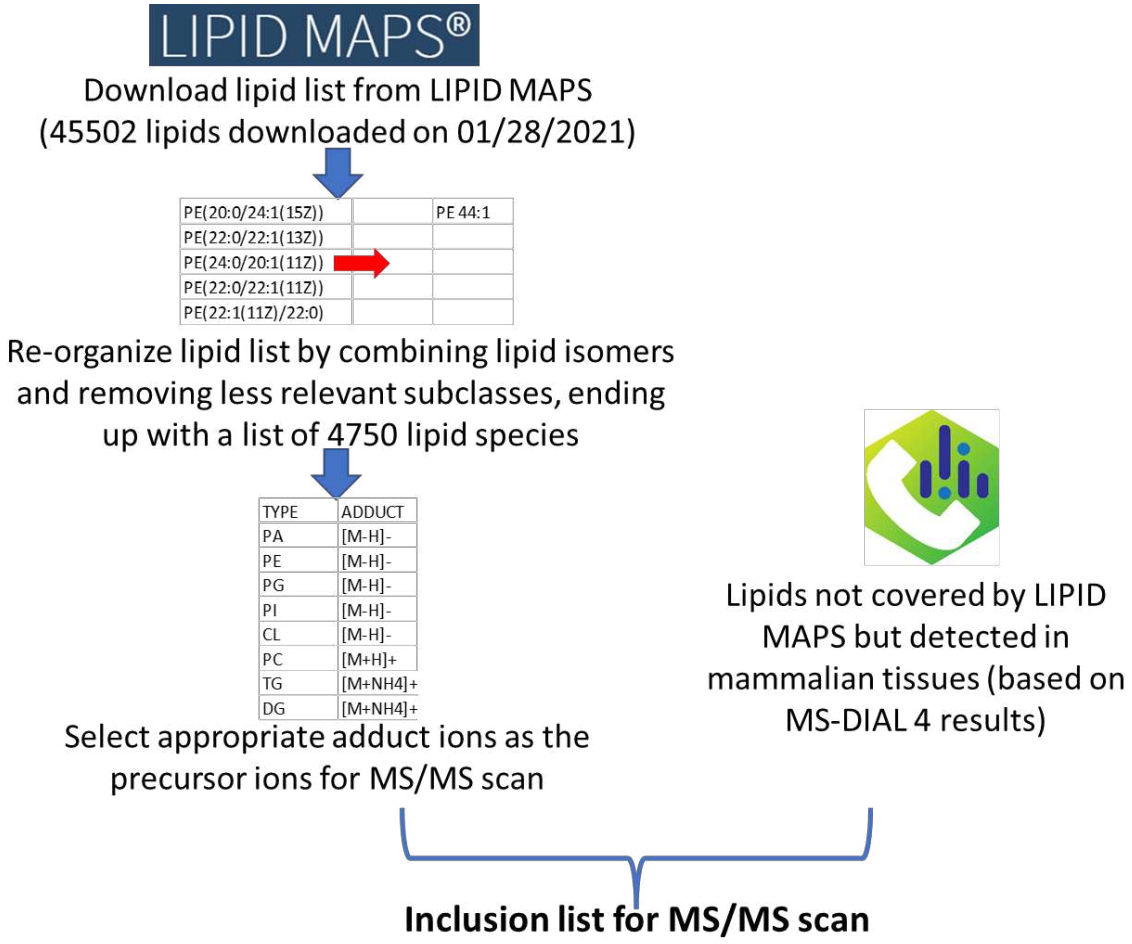

Figure 1 Construction of MS/MS inclusion list based on LIPID MAPS and lipidome atlas in MS-DIAL 4

"Less relevant subclasses" includes lipid subclasses that are not detected using current LC-MS workflow, such as saccharolipids, polyketides, and lipid subtypes that only include 1 or 2 lipids. Lipidome atlas information in MS-DIAL 4 was obtained from a previous publication[2].

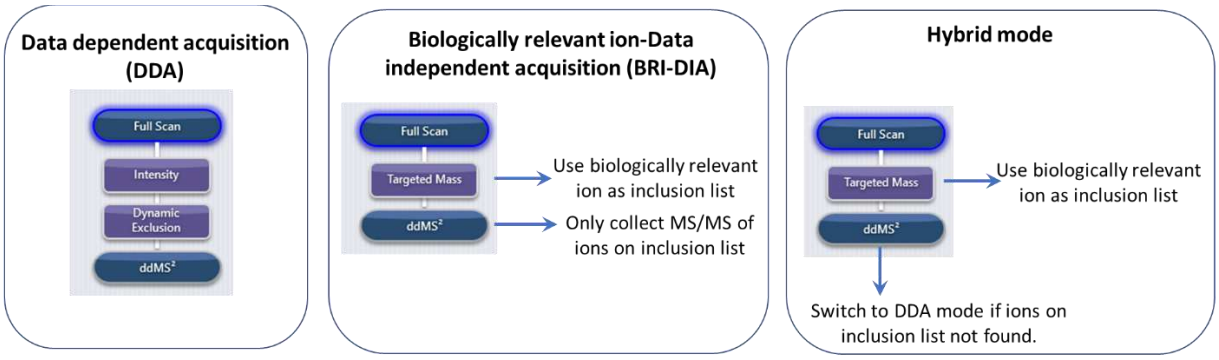

Figure 2 Description of three MS/MS scan workflow in lipidomic analysis. Inclusion list for targeted mass of MS/MS scan is included in Supplementary table 1.

a

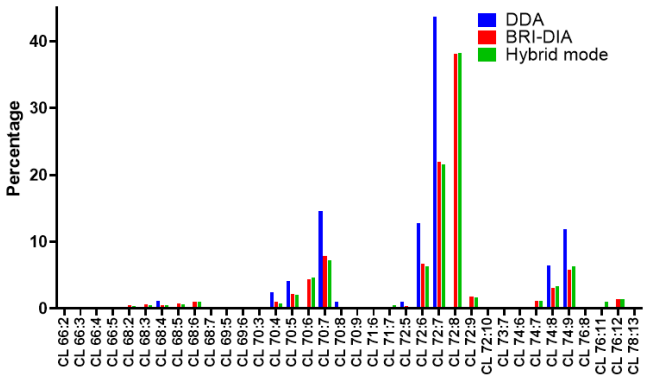

b

CL	CL acyl chain composition	DDA (CL %)	BRI-DIA (CL %)	Hybrid mode (CL %)
CL 66:2	CL 32:1_34:1	0.06	0.02	
CL 66:3	CL 16:0_16:0_18:1_18:2		0.05	
CL 66:4	CL 32:1_34:3, CL 32:2_34:2		0.07	0.07
CL 66:5	CL 16:1_16:1_16:1_18:2		0.1	0.11
CL 68:2	CL 16:0_18:1_16:0_18:1		0.44	0.41
CL 68:3	CL 16:0_18:1_16:0_18:2		0.61	0.49
CL 68:4	CL 16:0_18:1_16:1_18:2	1.07	0.54	0.51
CL 68:5	CL 16:1_16:1_18:1_18:2		0.74	0.68
CL 68:6	CL 16:1_16:1_18:2_18:2		1.02	0.96
CL 68:7	CL 14:1_18:2_18:2_18:2	0.19	0.08	0.09
CL 69:5	CL 15:1_18:1_18:1_18:2	0.22		
CL 69:6	CL 34:3_35:3	0.24		
CL 70:3	CL 16:0_18:1_18:1_18:1		0.07	0.13
CL 70:4	CL 16:0_18:1_18:1_18:2	2.39	1.03	0.78
CL 70:5	CL 16:0_18:2_18:1_18:2, CL 16:1_18:1_18:1_18:2	4.09	2.19	2.06
CL 70:6	CL 16:1_18:2_18:1_18:2		4.31	4.68
CL 70:7	CL 16:1_18:2_18:2_18:2	14.63	7.93	7.26
CL 70:8	CL 16:2_18:2_18:2_18:2	0.97		
CL 70:9	CL 33:2_37:7	0.23		
CL 71:6	CL 17:1_18:2_18:1_18:2			0.25
CL 71:7	CL 17:1_18:2_18:2_18:2			0.48
CL 72:5	CL 18:1_18:1_18:1_18:2	0.99	0.33	
CL 72:6	CL 18:1_18:2_18:1_18:2	12.75	6.74	6.31
CL 72:7	CL 18:1_18:2_18:2_18:2	43.64	21.98	21.52
CL 72:8	CL 18:2_18:2_18:2_18:2		38.12	38.22
CL 72:9	CL 16:1_20:4_18:2_18:2, CL 18:2_18:2_18:2_18:3		1.84	1.69
CL 72:10	CL 36:4_36:6	0.26		
CL 73:7	CL 37:3_36:4			0.13
CL 74:6	CL 18:1_18:1_18:1_20:3		0.18	
CL 74:7	CL 18:1_18:2_18:1_20:3		1.13	1.07
CL 74:8	CL 18:1_18:2_18:2_20:3	6.41	3.11	3.27
CL 74:9	CL 18:2_18:2_18:2_20:3	11.85	5.81	6.3
CL 76:8	CL 38:3_38:5, CL 38:4_38:4		0.05	0.07
CL 76:11	CL 18:1_18:2_18:2_22:6			0.95
CL 76:12	CL 18:2_18:2_18:2_22:6		1.44	1.42
CL 78:13	CL 38:5_40:8		0.07	0.07

Figure 3 The comparision of cardiolipi n composition determined by using three MS/MS scan methods. CL, cardiolipin. Bar graph (**a**) and table (**b**) of percentages of CL species. The percentage was determined by using the peak area values of each lipid species identified based on MS/MS spectrum collected using three different MS/MS scan methods. CLs highlighted in blue were identified using DDA method but not BRI-DIA or hybrid mode. CLs highlighted in green were not identified by DDA, but were identified using the other two methods.

a

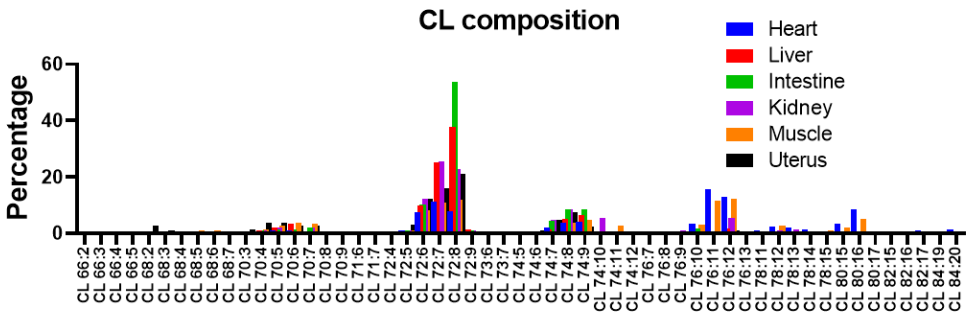

b

CL	CL acyl chain composition	Heart	Liver	Intestine	Kidney	Muscle	Uterus
CL 66:2	CL 32:1_34:1	0.01	0.03			0.06	
CL 66:3	CL 34:1_32:2		0.05		0.06		
CL 66:4	CL 32:2_34:2		0.06			0.24	
CL 66:5	CL 32:2_34:3		0.08			0.24	
CL 68:2	CL 16:0_18:1 16:0_18:1	0.32	0.46	0.54	0.19	0.61	2.93
CL 68:3	CL 16:0_18:1 16:0_18:2	0.23	0.43	0.21	0.31		1.26
CL 68:4	CL 14:0_18:1 18:1_18:2	0.15	0.42		0.31	0.67	0.71
CL 68:5	CL 14:0_18:2 18:1_18:2 (heart, liver,kidney), CL 16:1_16:1_18:1_18:2 (muscle)	0.18	0.48	0.35	0.50	1.20	0.45
CL 68:6	CL 14:0_18:2 18:2_18:2 (intestine, kidney), CL 16:1_16:1_18:2_18:2 (liver, muscle)		0.57	0.42	0.44	1.15	0.31
CL 68:7	CL 14:1_18:2 18:2_18:2		0.08				
CL 70:3	CL 16:0_18:1 18:1_18:1	0.17	0.17			0.28	1.28
CL 70:4	CL 16:0_18:1 18:1_18:2		1.02	1.07	1.08	1.28	3.71
CL 70:5	CL 16:0_18:2 18:1_18:2 (heart, intestine, kidney, uterus), CL 16:1_18:1_18:1_18:2 (liver, muscle)	1.09	2.02	1.35	2.08	2.69	3.89
CL 70:6	CL 16:1_18:2 18:1_18:2	1.00	3.42	1.48		3.67	2.88
CL 70:7	CL 16:1_18:2 18:2_18:2	0.66		2.14	2.13	3.40	2.95
CL 70:8	CL 16:2_18:2 18:2_18:2	0.04		0.11	0.14		
CL 70:9	CL 16:1_16:1 18:2_20:5					0.32	
CL 71:6	CL 17:1_18:2 18:1_18:2	0.10	0.39		0.20	0.27	
CL 71:7	CL 17:1_18:2 18:2_18:2				0.19		
CL 72:4	CL 18:1_18:1 18:1_18:1	0.16				0.14	0.59
CL 72:5	CL 18:1_18:1 18:1_18:2	1.24	0.63	1.25	1.17	1.12	3.11
CL 72:6	CL 18:1_18:2 18:1_18:2	7.39	9.80	10.16	12.42	8.24	12.14
CL 72:7	CL 18:1_18:2 18:2_18:2	11.45	25.33		25.48	10.87	15.99
CL 72:8	CL 18:2_18:2 18:2_18:2	7.93	37.60	53.89	22.68	11.97	21.25
CL 72:9	CL 18:2_18:2 18:2_18:3 (intestine, kidney), CL 16:1_20:4_18:2_18:2 (liver)		1.46	1.05	1.22		
CL 73:6	CL 36:3_37:3	0.10					
CL 73:7	CL 37:3_36:4	0.11	0.27	0.45	0.26		
CL 74:5	CL 36:2_38:3	0.08					
CL 74:6	CL 18:1_18:1 18:1_20:3	0.52		0.71	0.54	0.45	1.02
CL 74:7	CL 18:1_18:2 18:1_20:3	2.14	1.53	4.51	4.65		4.77
CL 74:8	CL 18:1_18:2 18:2_20:3 (heart, liver, intestine, kidney), CL 18:1_18:2_18:1_20:4 (muscle, uterus)	3.71	5.19	8.45	8.49	3.77	7.46
CL 74:9	CL 18:2_18:2 18:2_20:3 (heart, liver), CL 18:1_18:2_18:2_20:4 (intestine, muscle, uterus)	4.28	6.49	8.62		4.73	2.39
CL 74:10	CL 18:2_18:2 18:2_20:4				5.36		
CL 74:11	CL 16:1_18:2 18:2_22:6 (heart, muscle), CL 18:2_18:2_18:2_20:5 (intestine)	0.72		0.36		2.78	
CL 74:12	CL 34:4_40:8 (heart), CL 16:2_18:2_18:2_22:6 (muscle)	0.05				0.29	
CL 76:7	CL 38:3_38:4	0.06		0.12			
CL 76:8	CL 18:1_20:3_18:1_20:3 (heart, kidney), CL 38:3_38:5 (liver), CL 38:4_38:4 (uterus)	0.34	0.09		0.62		0.65
CL 76:9	CL 38:4_38:5				1.07		
CL 76:10	CL 18:1_18:2 18:1_22:6 (heart, muscle, uterus), CL 18:0_20:4_18:2_20:4 (intestine)	3.54		1.60		3.15	2.50
CL 76:11	CL 18:1_18:2 18:2_22:6	15.61				11.54	
CL 76:12	CL 18:2_18:2 18:2_22:6 (heart, liver, kidney, muscle, uterus), CL 18:2_20:4_18:2_20:4 (intestine)	12.89	1.86	0.89	5.43	12.38	0.93
CL 76:13	CL 18:2_18:3 18:2_22:6	0.27					
CL 78:11	CL 18:1_20:3 18:1_22:6	1.05				0.84	
CL 78:12	CL 18:1_20:3 18:2_22:6	2.57		0.16	1.19	2.82	0.47
CL 78:13	CL 18:2_20:3 18:2_22:6	2.26	0.08	0.09	1.48		
CL 78:14	CL 18:2_20:4_20:4_20:4	1.49					
CL 78:15	CL 16:1_22:6_18:2_22:6	0.39				0.91	
CL 80:15	CL 18:1_22:6_18:2_22:6	3.41				2.09	
CL 80:16	CL 18:2_22:6_18:2_22:6	8.61			0.30	5.13	
CL 80:17	CL 18:2_22:6_18:3_22:6	0.18					
CL 82:15	CL 42:7_40:8	0.18					
CL 82:16	CL 18:1_22:6_20:3_22:6	0.55					
CL 82:17	CL 18:2_22:6_20:3_22:6	1.04					
CL 84:19	CL 18:1_22:6_22:6_22:6	0.40					
CL 84:20	CL 18:2_22:6_22:6_22:6	1.33				0.70	

Figure 4 The use of MS/MS inclusion list allows consistent identification of major cardiolipin species in various mouse tissues. Bar graph (**a**) and table (**b**) of the percentage of CL molecular species and acyl chain composition. CL, cardiolipin. The percentage of each CL species was determined by using the peak area values of each lipid species identified based on MS/MS spectrum collected using hybride mode. When acyl chain composition varied with tissue type, the associated tissue type was indicated.

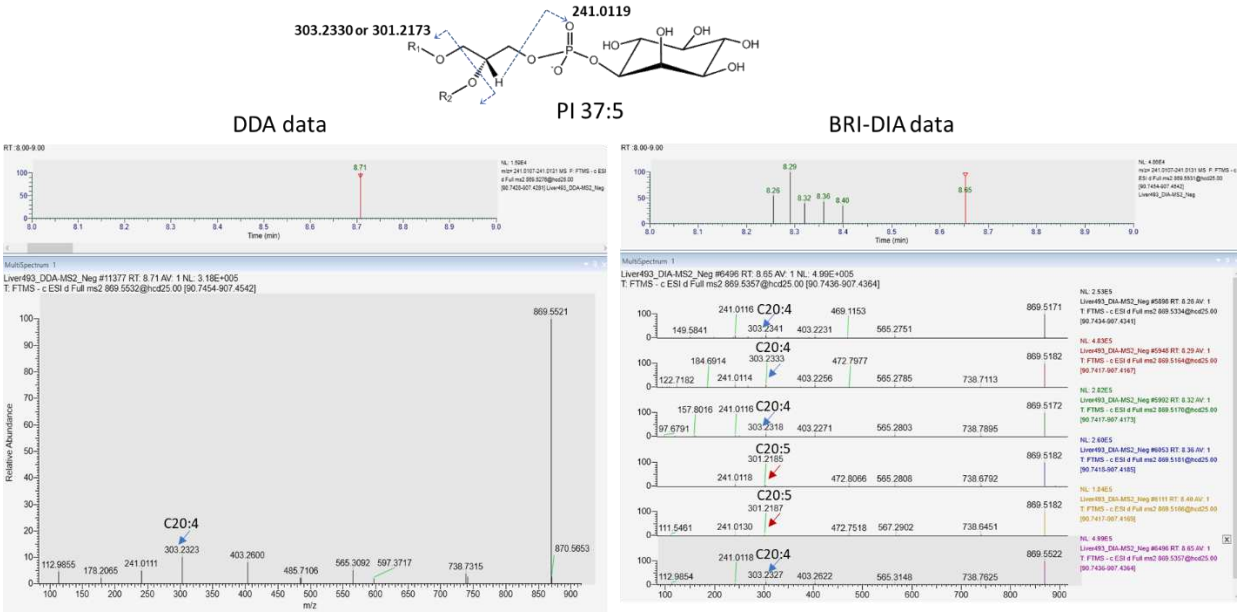

Figure 5 Representative MS/MS spectra of PI 37:5 in DDA and BRI-DIA data. PI, phosphatidylinositol. 241.0119 is the theoretical m/z of the polar head group [phosphoinositol – H_2O – H]$^-$. 303.2330 or 301.2173 is the theoretical m/z of fatty acids C20:4 or C20:5 negative ions.

Performance evaluation	DDA_pos	BRI-DIA_pos	Hybrid mode_pos	DDA_neg	BRI-DIA_neg	Hybrid mode_neg
Total number of identified lipids	692	476	500	383	323	355
Number of identified lipids with big mass error (>4ppm)	119 (17.2%)	40 (8.4%)	53 (10.6%)	59 (15.4%)	47 (14.6%)	42 (11.8%)
Number of identified lipids with wrong retention time or redundancy	59 (8.5%)	19 (4.0%)	21 (4.2%)	14 (3.7%)	4 (1.2%)	10 (2.8%)
Number of identified lipids with poor MS/MS information	50 (7.2%)	4 (0.8%)	15 (3.0%)	37 (9.7%)	1 (0.3%)	19 (5.4%)

Table 1 Comparison of the performance of different MS/MS scan methods in lipidomic analysis of mouse liver

Performance evaluation	DDA	BRI-DIA	Hybrid mode
Total number of identified lipids	737	684	695
Number of unique lipids	584 (79%)	585 (86%)	576 (83%)

Table 2 Total number of unique lipids identified by combining lipids detected in positive and negative ion mode.

Lipid subclass	DDA	BRI-DIA	Hybrid Mode
TG	139	154	147
PC	84	90	77
PE	44	46	46
EtherPE	27	27	28
DG	27	25	25
EtherPC	27	12	22
SM	26	21	23
LPC	25	27	26
LPE	23	16	17
CL	20	29	27
PI	17	23	21
Cer_NS	17	9	18
PS	17	18	16
CAR	16	12	13
PG	11	21	19
HexCer_NS	9	3	4
PA	8	6	6
CE	6	5	5
OxPE	5	7	3
EtherLPE	4	3	3
HexCer_NDS	4	3	2
Others	28	28	28

Table 3 Summary of lipid species identified by using different MS/MS scan workflow. TG, Triglyceride; PC, Phosphatidylcholine; PE, Phosphatidylethanolamine; EtherPE, Ether-linked phosphatidylethanolamine; DG, Diglyceride; EtherPC, Ether-linked phosphatidylcholine; SM, Sphingomyelin; LPC, Lysophophatidylcholine; LPE, Lysophosphatidylethanolamine; CL, Cardiolipin; PI, Phosphatidylinositol; Cer_NS, Ceramide non-hydroxyfatty acid-sphingosine; PS, Phosphatidylserine; CAR, Acyl carnitine; PG, Phosphatidylgylcerol; HexCer_NS, Hexosylceramide non-hydroxyfatty acid-sphingosine; PA, Phosphatidic acid; CE, Cholesteryl ester; OxPE, Oxidized phosphatidylethanolamine; EtherLPE, Ether-linked lysophosphatidylethanolamine; HexCer_NDS, Hexosylceramide non-hydroxyfatty acid-dihydrosphingosine. For simplicity, 23 lipid subclasses in which fewer than 3 lipids were identified using the current method, were summarized as “Others”.

Supplementary figure and tables

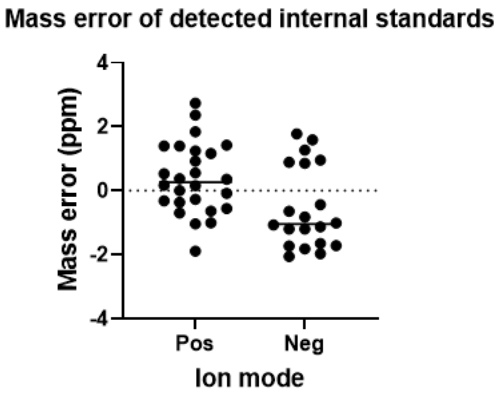

Supplementary figure 1 The mass error of internal standards detected in full scan over 3 days

Supplementary table 1 Inclusion list (positive and negative ion mode) used in BRI-DIA and hybrid mode

Supplementary table 2 Lipids identified by MS-DIAL in data collected using DDA, BRI-DIA and hybrid mode methods.

References

1. Han, X., The emerging role of lipidomics in prediction of diseases. *Nat Rev Endocrinol* **2022**.
2. Tsugawa, H.; Ikeda, K.; Takahashi, M.; Satoh, A.; Mori, Y.; Uchino, H.; Okahashi, N.; Yamada, Y.; Tada, I.; Bonini, P.; Higashi, Y.; Okazaki, Y.; Zhou, Z.; Zhu, Z. J.; Koelmel, J.; Cajka, T.; Fiehn, O.; Saito, K.; Arita, M.; Arita, M., A lipidome atlas in MS-DIAL 4. *Nat Biotechnol* **2020,** *38* (10), 1159-1163.
3. Zullig, T.; Trotzmuller, M.; Kofeler, H. C., Lipidomics from sample preparation to data analysis: a primer. *Anal Bioanal Chem* **2020,** *412* (10), 2191-2209.
4. Han, X.; Gross, R. W., The foundations and development of lipidomics. *J Lipid Res* **2022,** *63* (2), 100164.
5. Heiles, S., Advanced tandem mass spectrometry in metabolomics and lipidomics-methods and applications. *Anal Bioanal Chem* **2021,** *413* (24), 5927-5948.
6. Meikle, T. G.; Huynh, K.; Giles, C.; Meikle, P. J., Clinical lipidomics: realizing the potential of lipid profiling. *J Lipid Res* **2021,** *62*, 100127.
7. Xu, T.; Hu, C.; Xuan, Q.; Xu, G., Recent advances in analytical strategies for mass spectrometry-based lipidomics. *Anal Chim Acta* **2020,** *1137*, 156-169.
8. Hutchins, P. D.; Russell, J. D.; Coon, J. J., Accelerating Lipidomic Method Development through in Silico Simulation. *Anal Chem* **2019,** *91* (15), 9698-9706.
9. Ding, M.; Rexrode, K. M., A Review of Lipidomics of Cardiovascular Disease Highlights the Importance of Isolating Lipoproteins. *Metabolites* **2020,** *10* (4).
10. Lamichhane, S.; Sen, P.; Alves, M. A.; Ribeiro, H. C.; Raunioniemi, P.; Hyotylainen, T.; Oresic, M., Linking Gut Microbiome and Lipid Metabolism: Moving beyond Associations. *Metabolites* **2021,** *11* (1).
11. Masoodi, M.; Gastaldelli, A.; Hyotylainen, T.; Arretxe, E.; Alonso, C.; Gaggini, M.; Brosnan, J.; Anstee, Q. M.; Millet, O.; Ortiz, P.; Mato, J. M.; Dufour, J. F.; Oresic, M., Metabolomics and lipidomics in NAFLD: biomarkers and non-invasive diagnostic tests. *Nat Rev Gastroenterol Hepatol* **2021,** *18* (12), 835-856.
12. Castellanos, D. B.; Martin-Jimenez, C. A.; Rojas-Rodriguez, F.; Barreto, G. E.; Gonzalez, J., Brain lipidomics as a rising field in neurodegenerative contexts: Perspectives with Machine Learning approaches. *Front Neuroendocrinol* **2021,** *61*, 100899.
13. Pan, M.; Qin, C.; Han, X., Lipid Metabolism and Lipidomics Applications in Cancer Research. *Adv Exp Med Biol* **2021,** *1316*, 1-24.
14. Lv, J.; Zhang, L.; Yan, F.; Wang, X., Clinical lipidomics: a new way to diagnose human diseases. *Clin Transl Med* **2018,** *7* (1), 12.
15. Vvedenskaya, O.; Holcapek, M.; Vogeser, M.; Ekroos, K.; Meikle, P. J.; Bendt, A. K., Clinical lipidomics - A community-driven roadmap to translate research into clinical applications. *J Mass Spectrom Adv Clin Lab* **2022,** *24*, 1-4.
16. Zhang, L.; Zhu, B.; Zeng, Y.; Shen, H.; Zhang, J.; Wang, X., Clinical lipidomics in understanding of lung cancer: Opportunity and challenge. *Cancer Lett* **2020,** *470*, 75-83.
17. Breitkopf, S. B.; Ricoult, S. J. H.; Yuan, M.; Xu, Y.; Peake, D. A.; Manning, B. D.; Asara, J. M., A relative quantitative positive/negative ion switching method for untargeted lipidomics via high resolution LC-MS/MS from any biological source. *Metabolomics* **2017,** *13* (3).
18. Davies, V.; Wandy, J.; Weidt, S.; van der Hooft, J. J. J.; Miller, A.; Daly, R.; Rogers, S., Rapid Development of Improved Data-Dependent Acquisition Strategies. *Anal Chem* **2021,** *93* (14), 5676-5683.
19. Raetz, M.; Bonner, R.; Hopfgartner, G., SWATH-MS for metabolomics and lipidomics: critical aspects of qualitative and quantitative analysis. *Metabolomics* **2020,** *16* (6), 71.

20. Gillet, L. C.; Navarro, P.; Tate, S.; Rost, H.; Selevsek, N.; Reiter, L.; Bonner, R.; Aebersold, R., Targeted data extraction of the MS/MS spectra generated by data-independent acquisition: a new concept for consistent and accurate proteome analysis. *Mol Cell Proteomics* **2012,** *11* (6), O111 016717.
21. Gao, F.; McDaniel, J.; Chen, E. Y.; Rockwell, H. E.; Nguyen, C.; Lynes, M. D.; Tseng, Y. H.; Sarangarajan, R.; Narain, N. R.; Kiebish, M. A., Adapted MS/MS(ALL) Shotgun Lipidomics Approach for Analysis of Cardiolipin Molecular Species. *Lipids* **2018,** *53* (1), 133-142.
22. Bird, S. S.; Marur, V. R.; Sniatynski, M. J.; Greenberg, H. K.; Kristal, B. S., Serum lipidomics profiling using LC-MS and high-energy collisional dissociation fragmentation: focus on triglyceride detection and characterization. *Anal Chem* **2011,** *83* (17), 6648-57.
23. Surma, M. A.; Herzog, R.; Vasilj, A.; Klose, C.; Christinat, N.; Morin-Rivron, D.; Simons, K.; Masoodi, M.; Sampaio, J. L., An automated shotgun lipidomics platform for high throughput, comprehensive, and quantitative analysis of blood plasma intact lipids. *Eur J Lipid Sci Technol* **2015,** *117* (10), 1540-1549.
24. Willems, P.; Fels, U.; Staes, A.; Gevaert, K.; Van Damme, P., Use of Hybrid Data-Dependent and -Independent Acquisition Spectral Libraries Empowers Dual-Proteome Profiling. *J Proteome Res* **2021,** *20* (2), 1165-1177.
25. Guo, J.; Shen, S.; Xing, S.; Huan, T., DaDIA: Hybridizing Data-Dependent and Data-Independent Acquisition Modes for Generating High-Quality Metabolomic Data. *Anal Chem* **2021,** *93* (4), 2669-2677.
26. Lou, R.; Tang, P.; Ding, K.; Li, S.; Tian, C.; Li, Y.; Zhao, S.; Zhang, Y.; Shui, W., Hybrid Spectral Library Combining DIA-MS Data and a Targeted Virtual Library Substantially Deepens the Proteome Coverage. *iScience* **2020,** *23* (3), 100903.
27. Kitata, R. B.; Choong, W. K.; Tsai, C. F.; Lin, P. Y.; Chen, B. S.; Chang, Y. C.; Nesvizhskii, A. I.; Sung, T. Y.; Chen, Y. J., A data-independent acquisition-based global phosphoproteomics system enables deep profiling. *Nat Commun* **2021,** *12* (1), 2539.
28. Kind, T.; Liu, K. H.; Lee, D. Y.; DeFelice, B.; Meissen, J. K.; Fiehn, O., LipidBlast in silico tandem mass spectrometry database for lipid identification. *Nat Methods* **2013,** *10* (8), 755-8.
29. Fahy, E.; Subramaniam, S.; Murphy, R. C.; Nishijima, M.; Raetz, C. R.; Shimizu, T.; Spener, F.; van Meer, G.; Wakelam, M. J.; Dennis, E. A., Update of the LIPID MAPS comprehensive classification system for lipids. *J Lipid Res* **2009,** *50 Suppl*, S9-14.
30. Fahy, E.; Cotter, D.; Byrnes, R.; Sud, M.; Maer, A.; Li, J.; Nadeau, D.; Zhau, Y.; Subramaniam, S., Bioinformatics for lipidomics. *Methods Enzymol* **2007,** *432*, 247-73.
31. Falabella, M.; Vernon, H. J.; Hanna, M. G.; Claypool, S. M.; Pitceathly, R. D. S., Cardiolipin, Mitochondria, and Neurological Disease. *Trends Endocrinol Metab* **2021,** *32* (4), 224-237.
32. Oemer, G.; Koch, J.; Wohlfarter, Y.; Alam, M. T.; Lackner, K.; Sailer, S.; Neumann, L.; Lindner, H. H.; Watschinger, K.; Haltmeier, M.; Werner, E. R.; Zschocke, J.; Keller, M. A., Phospholipid Acyl Chain Diversity Controls the Tissue-Specific Assembly of Mitochondrial Cardiolipins. *Cell Rep* **2020,** *30* (12), 4281-4291 e4.
33. Acehan, D.; Vaz, F.; Houtkooper, R. H.; James, J.; Moore, V.; Tokunaga, C.; Kulik, W.; Wansapura, J.; Toth, M. J.; Strauss, A.; Khuchua, Z., Cardiac and skeletal muscle defects in a mouse model of human Barth syndrome. *J Biol Chem* **2011,** *286* (2), 899-908.
34. Han, X.; Yang, K.; Yang, J.; Cheng, H.; Gross, R. W., Shotgun lipidomics of cardiolipin molecular species in lipid extracts of biological samples. *J Lipid Res* **2006,** *47* (4), 864-79.
35. Mazaleuskaya, L. L.; Salamatipour, A.; Sarantopoulou, D.; Weng, L.; FitzGerald, G. A.; Blair, I. A.; Mesaros, C., Analysis of HETEs in human whole blood by chiral UHPLC-ECAPCI/HRMS. *J Lipid Res* **2018,** *59* (3), 564-575.
36. Leaptrot, K. L.; May, J. C.; Dodds, J. N.; McLean, J. A., Ion mobility conformational lipid atlas for high confidence lipidomics. *Nat Commun* **2019,** *10* (1), 985.

37. Bowman, A. P.; Abzalimov, R. R.; Shvartsburg, A. A., Broad Separation of Isomeric Lipids by High-Resolution Differential Ion Mobility Spectrometry with Tandem Mass Spectrometry. *J Am Soc Mass Spectrom* **2017,** *28* (8), 1552-1561.
38. Kyle, J. E.; Zhang, X.; Weitz, K. K.; Monroe, M. E.; Ibrahim, Y. M.; Moore, R. J.; Cha, J.; Sun, X.; Lovelace, E. S.; Wagoner, J.; Polyak, S. J.; Metz, T. O.; Dey, S. K.; Smith, R. D.; Burnum-Johnson, K. E.; Baker, E. S., Uncovering biologically significant lipid isomers with liquid chromatography, ion mobility spectrometry and mass spectrometry. *Analyst* **2016,** *141* (5), 1649-59.

Supplementary Files

This is a list of supplementary files associated with this preprint. Click to download.

- Supplementarytable1.xlsx
- Supplementarytable2.xlsx